

C.P. No. 844

C.P. No. 844

LIBRARY
ROYAL AIRCRAFT ESTABLISHMENT
BEDFORD.



MINISTRY OF AVIATION

AERONAUTICAL RESEARCH COUNCIL

CURRENT PAPERS

The Role of Compressive Strain in the Load and Strain Fatigue Behaviour of H.46 at Room Temperature

By

G. P. Tilly, B.Sc., Ph.D., A.C.G.I., D.I.C.

LONDON: HER MAJESTY'S STATIONERY OFFICE

1966

Price 7s. 6d. net

June 1965

The role of compressive stress in the load and
strain fatigue behaviour of H.46
at room temperature

- by -

G. P. Tilly

SUMMARY

Constant load amplitude and constant strain amplitude fatigue tests have been conducted on an 11 per cent Cr steel (H.46) at frequencies of 7 c/hr and 10 c/min at room temperature. The rupture data of the two tests correlated closely for both frequencies in terms of maximum applied stress at 50 per cent life, but the constant strain amplitude data exhibited enhanced endurance in terms of strain range at this life. In general, constant load amplitude fatigue appeared to be more damaging than constant strain at this temperature.

The constant load amplitude fatigue tests accumulated tensile strain in a time dependent manner which was amenable to analysis by a technique originally developed for elevated temperature creep data. The rate of strain accumulation of repeated tension load fatigue and static tensile stress tests was slower than for fully reversed push-pull. Strain continued to accumulate in a tensile sense during push-pull tests at 7 c/hr despite excess compressive stresses which were as much as 8 per cent greater than the complementary tensile stresses, whilst cycles with 16.5 per cent excess compressive stress produced compressive strain accumulation. Repeated tension fatigue work-hardened the material and it became successively more resistant to deformation, whereas push-pull fatigue work-softened it and it became successively less resistant to deformation.

CONTENTS

	<u>Page</u>
1.0 Introduction	4
2.0 Experimental technique	5
2.1 Material	5
2.2 Programme	6
3.0 Results	6
3.1 Constant load amplitude fatigue tests	6
3.2 Constant strain amplitude fatigue tests	7
3.3 Effects of compressive mean stresses at 7 c/hr	8
3.4 Static constant tensile stress tests	8
4.0 Discussion	8
4.1 The accumulation of strain	8
4.2 The correlation of load and strain ranges with the rupture data	11
5.0 Conclusions	13
5.1	13
5.2	13
5.3	13
5.4	13
5.5	13
5.6	13
5.7	13
5.8	13
List of Symbols	14
Acknowledgements	14
References	15

Detachable abstract cards

TABLES

<u>No.</u>	<u>Title</u>	
I	Constant load amplitude push-pull fatigue properties of H.46 at room temperature	17
II	Constant strain amplitude fatigue properties of H.46 at room temperature	18
III	Constant load amplitude push-pull fatigue tests at variable stress ratios	19
IV	Static constant tensile stress tests	20

TABLES (cont'd)

<u>No.</u>	<u>Title</u>	<u>Page</u>
V	Values of strain exponents	20
VI	Some characteristic load and strain values	21

APPENDICES

<u>No.</u>	<u>Title</u>	
I	Definitions of terms used	22
II	Strain/time analysis	24

ILLUSTRATIONS

<u>Fig. No.</u>	<u>Title</u>
1	Schematic control system and push-pull fatigue test-piece
2	Constant load and constant strain amplitude fatigue stress/time rupture curves
3	Cumulative strain/time curves for push-pull fatigue at 7 c/hr
4	Total strain range/time curves for push-pull fatigue at 7 c/hr
5	Total and plastic strain/cycles rupture curves
6	Relaxation of total stress range during constant strain amplitude fatigue tests at c/hr
7	Effect of variation of push-pull stress ratio on fatigue endurance at 7 c/hr
8	Effect of variation of push-pull stress ratio on the cumulative strain/time curves at 7 c/hr
9	Effect of variation of push-pull ratio on total strain range/time curves
10	t^1 , t^9 and ϵ_0 cross-plot curves
11	Regenerated strain/time curves fitted to experimental data
12	Creep and fatigue cumulative strain/time curves
13	The behaviour of stress strain and load during high stress fatigue of H.46

1.0 Introduction

In recent investigations on an 11 per cent Cr steel (H.46), strain was shown to accumulate during slow repeated tension fatigue and to obey laws similar to those that describe static creep at elevated temperatures¹. This has also been shown to take place for either constant stress or constant load amplitude fatigue over a range of temperatures in investigations on a variety of materials^{2,3,4} (see Appendix I for definition of terms). The total strain range (ϵ_T) of H.46 repeated tension data was related to the number of cycles to failure (N) by a power law expression of the form

$$\epsilon_T N^a = \text{constant} \quad \dots(1)$$

where the exponent a is dependent on the testing conditions, which is similar to the extensively reported expression for constant strain amplitude fatigue. Fatigue due to repeated thermal shocks at the leading and trailing edges of gas turbine blades has been considered to be relevant to constant strain amplitude fatigue because the temperature differences between the mean value and the extreme values at the respective edges produce strains and stresses that are a function of such properties of the material as its coefficient of thermal expansion, modulus of elasticity, elastic range and plastic flow behaviour. A fatigue cycle is thus applied each time the turbine is operated. Isothermal, constant strain amplitude fatigue data (strain fatigue) has not given very good correlation with laboratory thermal fatigue test data, whereas constant load amplitude fatigue data (load fatigue) has apparently been more promising⁵.

In cases where it has been necessary to relate load fatigue and strain fatigue data, it has been assumed that the endurance of a push-pull load test is equal to that of a strain test which shakes down to a similar load level. This appears to be a reasonable first approximation, but requires closer examination because the strain and load ranges vary continuously during the two respective forms of test.

The room temperature load fatigue properties of this material (H.46) have been reported previously in some detail and attention was drawn to the interesting form that the cumulative strain/time curves assumed during push-pull and repeated tension fatigue⁶. This appeared important because the slow push-pull tests accumulated strain in a tensile sense, whereas it is usually assumed that equal tensile and compressive cycles are self-cancelling and result in little or no total strain accumulation. In one of the few relevant investigations to be reported, it was shown² that creep of an aluminium alloy at 300°F and 500°F was decreased by a decrease in the value of the tensile mean stress, and there was no observable creep accumulation during fully reversed push-pull fatigue tests at 300°F. Detailed push-pull data are usually viewed with some reserve however, because it is difficult to carry out compressive testing which is free from buckling and the resulting compressive instability can produce anomalous effects.

It appears that the conflicting evidence of previous investigations requires further examination in order to determine whether strain can accumulate during push-pull cyclic fatigue. Fatigue in service conditions is not necessarily fully reversed (zero mean stress) and is dependent upon the operating conditions which may impose a system that is composed of contributions by several forms of loading. The effects of mean stresses on the cumulative strain/time behaviour and rupture data are therefore of

some importance, as also is the relation of push-pull load cycling to constant strain amplitude cycling because it is not clear which test (if either) is most relevant to thermal fatigue.

2.0 Experimental technique

The fatigue tests were conducted at room temperature in a modified Amsler Vibrophore machine, the experimental technique having been described previously⁷. Additional care was taken to reduce the possibility of compressive buckling, and a test-piece with a reduced gauge length/diameter ratio was used. This re-designed test-piece was cylindrical with threaded ends and had a 0.1 in. gauge length which was 0.141 in. diameter. There were waisted portions at either end and 0.240 in. diameter shoulders (Figure 1.1). No compressive buckling was observed with this geometry and the push-pull rupture data correlated with data for a more slender test-piece.

The diametral strain was sensed by a differential transformer type transducer (designated 'A' in Figure 1.2) housed in a spring-mounted extensometer which has been described previously⁶. In the case of the load fatigue tests, the strain signal was sensed by this transducer and was amplified and continuously recorded against time on a strip chart (Figure 1.2). The load reversal limits were controlled by a second transducer (B) sited parallel to the main load spring of the testing machine. The signal from this transducer was fed to an amplifier control unit where cyclic reversal relays were controlled off adjustable limits.

In the case of the strain fatigue tests, the strain reversal limits were controlled by the strain transducer (A). The resulting signal was fed to the amplifier/control unit and the cyclic reversal relays were controlled by adjustable limits identical to those of the load control system. The tests were cycled between zero strain (corresponding to the 'as received' diameter) and a fixed tensile-strain limit. The load was sensed by the load transducer (B), and was recorded against time continuously on the strip chart recorder. In both types of test the actual load values were recorded manually off a load dynamometer supplied with the machine which was stated by the manufacturers to have an accuracy corresponding to $\frac{1}{4}$ per cent. The strip chart records of the test at 10 c/min were unsatisfactory because the rapid cyclic moment of the pen tended to damage the chart paper. The subsequent records were examined for general trends, but were not analysed in the same detail as the 7 c/hr test records which were more suitable for this system of recording.

Static constant tensile stress tests were conducted at room temperature in a creep machine developed by Wallis and Graham of N.G.T.E. The test-piece used was cylindrical with threaded ends and had a 1 in. gauge length of 0.178 in. diameter ($\frac{1}{40}$ sq in. cross-sectional area), and two ridges for locating a longitudinal extensometer. The loading system employed a cranked lever arm which ensured that the ratio of load to cross-sectional area was maintained constant and has previously been described in some detail¹.

2.1 Material

The material, a vacuum cast of H.46 steel was supplied as a 13 in. diameter forging, with a chemical analysis as follows:-

<u>Element</u>	<u>% Composition</u>	
Carbon	0.18	to 0.20
Manganese	0.79	0.90
Silicon	0.28	0.30
Sulphur	0.016	0.019
Phosphorus	0.013	0.017
Nickel	0.78	0.88
Chromium	11.0	11.4
Vanadium	0.38	0.41
Niobium	0.24	0.30
Molybdenum	0.55	0.64
Boron	0.0035	0.0040
Iron	Balance	

Blanks of $\frac{3}{8}$ in. square section were slit out in an axial direction. They were heat treated at 1150°C for 30 min and air-cooled followed by 3 hr at 640°C and air-cooled, to give a hardness of between 351 and 357 V.P.N.

2.2 Programme

Fatigue and static constant tensile stress tests were conducted on the above material at room temperature. Fully reversed push-pull load fatigue tests were at nominal frequencies of 7 c/hr and 10 c/min and tests with a range of push-pull stress ratios from -0.925 (tensile mean stress) to -1.165 (compressive mean stress) were at 7 c/hour. Continuous recordings were made of the diametral strain against time.

Repeated tension strain fatigue tests were conducted at the same two nominal frequencies and load was recorded against time.

Static constant tensile stress tests were conducted for comparison and longitudinal strain was recorded against time.

The respective applied stress and strain amplitudes were selected such that the failure times were between those of the monotonic tensile tests and about 100 hours. The first application of stress or strain was always in a tensile sense.

3.0 Results

3.1 Constant load amplitude fatigue tests

The push-pull load fatigue rupture data were expressed as maximum applied stress against both time to failure and cycles to failure in Figure 2. The data for each frequency were clearly separated on the time

base, but exhibited little frequency effect on the cycle base although the latter comparison was partially obscured because the region of overlap of the two frequencies was limited. (Previous data have shown that there is a small increase in cyclic endurance with increase in frequency under these testing conditions⁶.) The curves exhibited no tendency to flatten out to a conventional fatigue limit within the range of endurances investigated and could be described adequately by straight lines.

The diametral deformation, of the 7 c/hr tests is expressed as cumulative diametral strain (the total contemporary strain at maximum tensile stress) and plotted against time in Figure 3. The curves all exhibit an increase in tensile strain accumulation with increasing time and appear to form a regular family with an appearance similar to that of tensile creep. The strain records were examined in further detail and the total strain ranges (or amplitudes) plotted against time (Figure 4). The resulting records are similar to the cumulative strain/time curves and exhibit an increase in strain range with increase in time.

3.2 Constant strain amplitude fatigue tests

The loads required to cycle the test-piece between the 'as received' zero and a given tensile strain were compressive as well as tensile, because the first tensile application produced a permanent strain such that it was necessary to apply a compressive load to restore it to its datum length as illustrated schematically in Figure 13. The nature of the subsequent cycles quickly reverted to that of a push-pull type load test, the compressive loads being ~5 per cent greater than the complementary tensile loads. Repeated tension strain fatigue cycling is usually considered to be effectively the same loading condition as fully reversed strain having the same total range, because it has been shown that both shake down to the same load ranges and produce fractures in equal durations⁴.

The rupture data were expressed logarithmically as total strain range against number of cycles to failure, and as the calculated plastic strain range against number of cycles to failure (Figure 5). This latter value was calculated from the equation

$$\epsilon_p = \epsilon_T - \frac{\sigma}{E} \quad \dots(2)$$

where

- ϵ_p = plastic strain range
- ϵ_T = total strain range
- σ = total stress range at 50 per cent life
- E = modulus of elasticity

usually applied to this type of test data. The data were rather scattered and difficult to interpret quantitatively but could be represented by straight lines according to the generally accepted power law expression (1). There was a limited region of overlap between test points of the 7 c/hr and the 10 c/min applied frequencies, but it was sufficient to reveal a marked speed effect whereby an increase in applied frequency at a given total or plastic strain range resulted in an increased cyclic endurance. The slopes (α) of the 'best fit' lines through the total strain data were -0.485 and -0.407 for the respective frequencies whereas the slopes (k) of the plastic strain data were both -0.59.

The stress data from six of the 7 c/hr tests were expressed as stress-range/cycles curves (Figure 6) and it can be seen that the stress ranges decreased continuously during the fatigue lives.

3.3 Effects of compressive mean stresses at 7 c/hr

The effect of various compressive mean stresses on the rupture endurance at 7 c/hr is illustrated in Figure 7. Tests conducted with 63.0 t/in² maximum tensile stress, but with compressive stresses in the range -58.0 t/in² to -73.4 t/in², produced little effect on the endurance as compared with a fully reversed test at ±63.0 t/in², whereas tests conducted with a compressive stress of -63.0 t/in² and higher tensile stresses, exhibited reduced endurances.

The cumulative strain/time curves are illustrated in Figure 8. The curves all exhibit a first quarter-cycle strain of ~3 per cent because this was the value produced by the common first tensile quarter-cycle load of 63.0 t/in², (the strains in Figure 8 were plotted against time as opposed to number of cycles, and the first quarter-cycle strain was represented by the first point on each curve). Increases in the compressive stress to -68.15 t/in² progressively decreased the rate of tensile strain accumulation. A test at $\begin{matrix} +63.0 \\ -70.65 \end{matrix}$ t/in² produced an unstable accumulation with a 'compressive kink' at about 12 hr, whilst a further increase in compressive stress to $\begin{matrix} +63.0 \\ -73.4 \end{matrix}$ t/in² produced an all-compressive strain accumulation.

Tests with increased tensile stress $\begin{pmatrix} +68.15 \\ -63.0 \end{pmatrix}$ t/in² exhibit a high first quarter-cycle tensile strain and the specimen subsequently accumulated strain at a more rapid rate than for ±63.0 t/in² whereas tests at a similar stress ratio (-0.92), but with decreased compressive stress $\begin{pmatrix} +63.0 \\ -58.0 \end{pmatrix}$ t/in² exhibit no significant change. The total strain range/time curves exhibit trends similar to those of the fully reversed push-pull tests, but are not separated into a clearly defined family as in the former case (Figure 9).

3.4 Static constant tensile stress tests

Static constant tensile stress creep tests were conducted such that failures were produced between about 1 and 100 hours. The stresses were expressed as nominal values i.e., initial load divided by cross-sectional area, and the longitudinal strains over a 1 in. gauge length were plotted against time in Figure 12.1. True stresses (contemporary load divided by contemporary cross-sectional area) were calculated and listed in Table IV.

4.0 Discussion

4.1 The accumulation of strain

The cumulative strain/time curves of the 7 c/hr push-pull fatigue tests exhibit tensile strain accumulations which have a similar appearance to those of tensile creep tests at elevated temperatures. Additional evidence of this trend is exhibited by the strain fatigue tests in which

5 per cent excess compressive load was required to maintain the strain amplitude constant, and by the variable stress ratio tests in which strain accumulation was tensile despite compressive mean stresses. In the latter case, the strain continued to accumulate tensile-wise for as much as 8 per cent excess compressive stress i.e., $\frac{+63.0}{-70.65}$ t/in² and it is interesting to note that this is nearly an order of magnitude greater than the excess tensile true stress produced by the changes in cross-sectional area at the maximum tensile and compressive loads. This difference in cross-sectional area is induced by the tensile and compressive strains and is related to the total strain range e.g., a test at ± 63.0 t/in² nominal stress was calculated to be $\frac{+63.45}{-62.55}$ t/in² true stress, at 50 per cent life.

The family of strain/time curves were analysed by a technique originally developed and applied to constant stress creep by Graham and Wallis^{9,10} (Appendix II). In this analysis, the curves were separated into a three-term expression of the form

$$\epsilon = \epsilon_0 + at + bt^a \quad \dots(3)$$

and the 1 per cent strain intercepts of the t^1 and t^a terms were related to the applied stress by the expression

$$\sigma = ct^{\frac{1}{b}} \quad \dots(4)$$

where

ϵ strain

ϵ_0 first cycle loading strain

t time

σ stress

a, b, c constants

The time and stress exponents are members of a discrete series and the particular numerical values used in Equations (3) and (4) represent the terms which were operative for this material and testing condition. The strain/time curves were regenerated from these two expressions and compared with the experimental data (Figure 11). It is clear that the analysis fits very closely for these testing conditions and appears to be a valid and useful method of describing the data.

The strain/time records show that after the first application of tensile stress, the subsequent equal and opposite compressive stress was insufficient to restore the specimen to its original dimensions, and the fully reversed push-pull cycling enhanced the rate of strain accumulation compared with that produced by repeated tension fatigue at an equal maximum applied stress (Figure 12.2). The different behaviour of the push-pull and repeated tension strain accumulations appears to be due to the reversal of stresses producing an enhanced ductility. This is supported by the marked difference in behaviour of the total strain range/time curves of the

push-pull and repeated tension tests illustrated in Figure 12.3. The push-pull strain range in the example was 1.2 per cent in the first full cycle and subsequently increased continuously throughout the fatigue life (work-softened) whereas the repeated tension strain range decreased during the first few cycles (work-hardened) from 0.2 per cent to 0.128 per cent, remained fairly constant during most of the test, but markedly increased again immediately prior to fracture. It appears then, that the material work-softens and becomes successively less resistant to deformation during the push-pull fatigue test whereas it work-hardens and becomes successively more resistant during repeated tension fatigue testing.

In general, the application of fatigue cycles may either harden or soften the structure depending upon its initial condition. A material in an initially hard condition e.g., cold rolled, can become softer after the application of a number of fatigue cycles such that the resistance to deformation decreases, whereas a material in an initially soft condition e.g., annealed, becomes progressively harder, and more resistant to deformation^{4, 11}. (The H.46 steel used in this investigation was heat treated to give a hardness of 350 to 357 V.P.N. and was therefore in a comparatively hard condition.) The work-softening behaviour in the push-pull fatigue tests may be explained in terms of the Bauschinger effect whereby the application of stress in one direction lowers the yield stress in the opposite direction. Repeated stress reversals can produce stress/strain hysteresis loops with marked plastic deformation during fatigue tests of up to 100 hr duration, whereas repeated stresses in one direction work-harden the material and raise the yield stress in that direction such that there is very little plastic deformation and the stress range becomes almost wholly elastic⁶. A material subjected to a prior history of repeated tension stresses in this manner is therefore more resistant to deformation than one subjected to reversed stresses. Unidirectional loading does not prohibit deformation completely however, and it can be seen that repeated tension load fatigue produces cumulative strain but at a lower rate (Figure 12.2). Repeated tension stress fatigue also produces cumulative strain provided the stresses are high enough¹.

The tests conducted with a range of mean stresses demonstrate that a comparatively large compressive stress is required to inhibit the tensile strain accumulation. The strain fatigue tests exhibit similar behaviour to the extent that tensile deformation was produced more easily than compressive deformation, i.e., in order to prohibit the accumulation of strain, it was necessary to apply compressive loads which were about 5 per cent greater than the tensile loads. At the same time, the total stress range decreased continuously as the material work-softened and successively less stress was required in the two respective directions to maintain it constant.

Mathematical analyses of the effects of fatigue loading on the strain accumulation at higher temperatures have usually been based on tensile creep and fatigue data. Such approaches often assume that a repeated tension test produces a creep curve characterised by an equivalent creep stress which is less than the maximum cyclic stress e.g., Reference 12. This approach is only supported by data of tests at the conventional creep temperatures however, and fails to predict the behaviour at lower temperatures where the stress to produce creep failure in a given time exceeds that to produce fatigue failure⁷. In addition, tensile and compressive creep characteristics are often assumed to be equal and opposite, which is not always true in practice because some materials

exhibit less resistance to tensile creep whereas others exhibit less resistance to compressive creep¹³. It is clear that if the strain accumulation produced during push-pull fatigue tests is viewed as a balance between tensile and compressive strain, the material in these room temperature tests is significantly less resistant to tensile stress and mathematical expressions which successfully described the components of the effect require different constants for tension and compression. The room temperature strain accumulation appears to be a form of creep as defined by the time-dependent deformation because the strain/time curves can be described by the same general equation as that for high temperature constant load creep, but this does not imply that the deformation mechanisms invoked by the high and low temperature conditions are identical.

The longitudinal strain/time curves relevant to static constant tensile stress tests (Figure 12.1) also exhibit strain accumulation, but at a lower rate than those of push-pull. The values of the stresses required to produce this time-dependent deformation were very high and the stress/time rupture curve had a very low slope such that a small change in stress produced a very great change in the time to failure. The scatter band appeared to exceed the decrease in stress related to this stress/time slope and it was difficult to correlate stress and time. The data exhibited well defined tensile strain accumulation despite the fact that the tests were at a constant stress (decreasing load). The strain/time curves appear on inspection to be composed mostly of a very low term which is probably $t^{\frac{1}{31}}$ and there are fairly well defined $t^{\frac{1}{5}}$ and $t^{\frac{1}{3}}$ terms evident during the later stage of the tests. It is possible that for static tests each of the time exponents is identified with a deformation mode, and the $t^{\frac{1}{31}}$ term characterises a basically low temperature mode whereas the higher terms commonly exhibited by materials in the conventional creep range are characteristic of high temperature behaviour.

4.2 The correlation of load and strain ranges with the rupture data

The strain fatigue rupture data are compared with the load fatigue data in Figure 2, and it is clear that they correlate fairly closely on either stress/cycles or stress/time diagrams and can be described by straight lines which are common for the two forms of test. The respective slopes are very flat however ($\sim 1/32$ for the 7 c/hr data and $\sim 1/16$ for the 10 c/min data) and tend to exaggerate the success of the correlation.

Comparisons of the total strain range and calculated plastic strain range data of the respective tests at 50 per cent of the life to failure show that they do not correlate very closely on this basis, the strain fatigue exhibiting superior cyclic endurance at equal strain ranges (Figure 5). The correlation of the respective tests on a strain range/cycles basis is dependent upon the definition of the respective total strain ranges characterising the constant load amplitude tests. These are usually calculated at 50 per cent life on the assumption that the strain range has 'shaken down' and reached a more or less constant value at this stage of the test. Figure 4 and Table VI illustrate that this is not true for these tests, and the strain range to produce failure in some of the shorter endurance constant strain amplitude tests was never attained in the constant load tests at the same endurance, e.g., a failure occurred in a load fatigue test at ± 64.8 t/in² after 37 cycles during which time the strain range increased from 0.72 per cent to

1.3 per cent whereas a strain fatigue test would have required 2.8 per cent strain range to produce a life of 37 cycles. Individual comparisons at greater endurance were slightly more favourable and the load fatigue tests usually attained the strain range of the equivalent strain tests, but not necessarily at 50 per cent of the life to failure. The plastic strain range data ϵ_p could be related to the number of cycles to failure by the expression

$$\epsilon_p N^k = C \quad \dots(5)$$

which has been reported for a variety of materials and testing conditions⁸ although the exponents (k) calculated from Figure 5 were slightly higher than 0.5 which has been extensively reported to room temperature data (Table V). Higher room temperature values have been reported in investigations on copper⁴ and nickel¹⁴. Elevated temperature data usually exhibit values of k between 0.5 and 1 and this has been ascribed to the presence of time-dependent deformation or creep⁸. The increased value for H.46 may be ascribed to a similar mechanism because there is considerable evidence of time-dependent deformation within the testing range (Figure 12). The presence of a marked frequency effect in strain fatigue data is a characteristic of higher temperatures and is usually absent at room temperatures. It is unlikely, however, that this could have been produced by a deformation mechanism similar to that of conventional high temperature creep.

The stress/time relaxation curves in Figure 6 show that successively less load was required to maintain the strain range constant, and the material progressively work-softened during strain fatigue tests. It appears that there were two, and in some cases three stages of deformation analogous to primary, secondary, and tertiary creep, but there was no tendency in any of the tests to settle down to the steady-state shakedown condition that has been reported for many other materials.

It is clear that strain fatigue tests of H.46 apply successively less damaging cycles as measured by the stress range whereas load fatigue tests apply successively more damaging cycles because the total strain range increases and in addition, the cumulative strain produces a form of incremental collapse which results in a diminishing cross-sectional area to support the load. The apparent success of the 50 per cent life correlations on a stress basis may have been enhanced by the very low slopes of the S/N curves which produce a relatively insensitive comparison of the respective data. The load fatigue tests are affected less by changes in applied frequency than the strain fatigue tests, and it appears that the stress range is a less sensitive measure of the life to failure under these conditions. Both forms of test exhibit three stages of deformation, and produce continuous work-softening during the life to failure, but strain fatigue data may be considered as a measure of the resistance to strain cycles whereas load fatigue data is a measure of the resistance to load cycles. Components are usually designed from the 'as received' material behaviour, and fatigue is characterised by the first few reversals. Load fatigue has a more damaging effect than strain fatigue of H.46 at room temperature however, and the endurance is less than that of a strain fatigue test having an identical first cycle.

It appears that load fatigue data may be related to gas turbine operating conditions as effectively as the commonly used strain fatigue

provided the values of load and strain are recorded and analysed comprehensively. Push-pull load fatigue possibly has some additional merit because it produces more conservative rupture data as measured by the strain amplitude at either the first cycle or the 50 per cent life conditions. The cumulative strain or incremental collapse exhibited by this type of test may be relevant to the conditions produced by the combinations of thermal fatigue, interrupted centrifugal creep, and low stress bending vibrations which are present in gas turbine components but are not altogether simulated by other tests such as repeated bending or the thermal shock of tapered discs in fluidised beds.

5.0 Conclusions

5.1 Static tensile stress, constant load amplitude push-pull and constant load amplitude repeated tension fatigue tests on H.46 at room temperature exhibited time-dependent tensile strain accumulation.

5.2 Push-pull tests with compressive stresses that were between 0 and 8 per cent greater than the maximum tensile stresses also exhibited tensile strain accumulation. The increases in the excess compression stress decreased the tensile strain, and 16.5 per cent excess compression produced compressive strain accumulation.

5.3 The variations in compressive reversal stress of between +16.5 per cent and -8 per cent produced little change in the rupture endurance whereas an increase in tensile stress decreased it markedly.

5.4 Repeated tension fatigue testing work-hardened the material and decreased the strain range whereas fully reversed push-pull testing produced work-softening and increased the strain range. The introduction of compressive reversals enhanced the rate of tensile strain accumulation.

5.5 Constant strain amplitude fatigue rupture data exhibited a marked frequency effect whereby longer endurance were obtained at 10 c/min than at 7 c/hour. The constant load amplitude rupture data were considerably less sensitive to frequency at this temperature.

5.6 Constant load amplitude fatigue cycles appeared to have a more damaging effect than constant strain fatigue cycles.

5.7 The data from both types of fatigue test correlated closely on a maximum tensile stress basis (at 50 per cent life), whereas comparisons on a strain range basis showed that constant strain amplitude fatigue tests would give longer lives.

5.8 Compressive stress played a significant role in the fatigue behaviour of H.46 at room temperature and suggest that study of the role of compressive stress in the elevated temperature behaviour of gas turbine materials is needed.

List of Symbols

V.P.N.	Vickers pyramid hardness number
σ	applied stress
N	number of cycles to failure
t	time in hours
E	Young's modulus of elasticity
ϵ	strain
ϵ_0	first cycle loading strain
ϵ_T	total secondary strain range
ϵ_p	plastic strain range
α	total strain range exponent
K	plastic strain range exponent
β	stress exponent
κ	time exponent
a,b,c	material constants

ACKNOWLEDGEMENTS

The author gratefully acknowledges many helpful discussions with Mr. A. Graham, and would like to thank Mr. W. Gwenlan for setting up the fatigue tests and Mr. G. J. Bates for carrying out the heat treatment and hardness tests.

REFERENCES

- | <u>No.</u> | <u>Author(s)</u> | <u>Title, etc.</u> |
|------------|----------------------------------|---|
| 1 | G. P. Tilly | Effects of varied loading paths on fatigue endurance Part III - Some stress properties of H.46 at elevated temperatures.
A.R.C.26 056. C.P.788. June, 1964. |
| 2 | F. W. De Money,
B. J. Lazan | Dynamic creep and rupture properties of an aluminium alloy under axial, static and fatigue stress.
Proc. ASTM Vol. 54, 1954, p.769. |
| 3 | C. E. Feltner,
G. M. Sinclair | Cyclic strain induced creep of close packed metals.
Joint ASME-Inst. Mech.E.
International Creep Conference, October, 1963. |
| 4 | P. P. Benham | Low endurance fatigue of mild steel and an aluminium alloy.
J. of Inst. of Metals, Vol. 89, 1961, p.328. |
| 5 | J. T. Roberts | Comparative thermal fatigue tests on Nimonic 90 tapered disc specimens with and without internal air cooling.
N.G.T.E. Memorandum No. M.366.
A.R.C.25 322. September, 1963. |
| 6 | G. P. Tilly | Effects of varied loading paths on fatigue endurance Part II - Some load fatigue properties of H.46 at room temperature.
A.R.C.26 055. C.P. 787. March, 1964. |
| 7 | G. P. Tilly | Effects of varied loading paths on fatigue endurance Part I - Some load fatigue properties of Nimonic 90 at elevated temperatures.
A.R.C.25 880. C.P.786. December, 1963. |
| 8 | L. F. Coffin | Low cycle fatigue: a review.
Applied Materials Research Vol. 1(3), p.129.
October, 1962. |
| 9 | A. Graham | The phenomenological method in rheology.
Research (6) p.62, 1953. |
| 10 | K. F. A. Waller,
A. Graham | On the extrapolation and scatter of creep data.
A.R.C. Current Paper No. C.P.680. 1963. |

<u>No.</u>	<u>Author(s)</u>	<u>Title, etc.</u>
11	N. H. Polakowski, A. Palohoudhuri	Softening of certain cold-worked metals under the action of fatigue loads. Proc. ASTM Vol. 54, 1954, p.701.
12	G. Vidal	Sur le fluage périodique des alliages résistants à chaud. Rev. Met. Vol. 53, p.485, 1956.
13	O. K. Salmassy, O. L. Carlson, G. K. Nancy	An investigation of the interchange of tensile creep for compressive creep. Unpublished U.S. Report.
14	H. Majors	Thermal and mechanical fatigue of nickel and titanium. Trans. ASM Vol. 51, p.421, 1959.
15	J. T. P. Yao, W. H. Munse	Low cycle fatigue of metals - Literature Review. Welding Research Supplement Vol. 41 (4), p.1825, 1962.
16	K. F. A. Wallis	Contribution to the discussion of the Joint ASME-Inst. Mech.E. International Creep Conference. October, 1963.

TABLE I

Constant load amplitude push-pull fatigue properties
of H.46 at room temperature

Applied frequency	Applied stress (t/in ²)	Time to fracture, hr	Cycles to fracture	Total strain range $\epsilon_T\%$	Plastic strain range $\epsilon_P\%$
7 c/hr	±60.0	47.65	239	0.50	0.258
	±57.0	131.1	647	0.42	0.173
	±62.0	32.2	142	-	-
	±58.0	208.1	954	0.46	0.209
	±67.8	5.05	20	1.50	1.206
	±64.8	8.9	37	0.96	0.680
	±63.0	14.5	63	0.685	0.412
	±60.8	64.9	287	0.64	0.362
	±68.1	18.9	96	0.465	0.170
10 c/min	±60.4	0.7	397	0.62	0.36
	±55.0	1.9	1151	0.34	0.102
	±50.0	15.5	9907	0.285	0.069
	±48.6	15.85	10631	-	-
	±43.5	58.8	42038	-	-
	±58.0	1.55	919	0.616	0.364
	±53.0	7.7	4618	0.338	0.108
	±60.2	0.9	458	0.74	0.479
	±41.6	88.8	64524	-	-

TABLE II

Constant strain amplitude fatigue properties of
H.46 at room temperature

Applied frequency	Total applied strain range $\epsilon_T\%$	Time to fracture, hr	Cycles to fracture	Shakedown stress (t/in ²)	Plastic strain range $\epsilon_T\%$
7 c/hr	0.715	127.9	581	58.2	0.463
	0.856	90.05	394	60.5	0.594
	1.275	51.2	214	61.9	1.007
	1.545	12.65	55	64.9	1.264
	0.565	128.1	610	57.1	0.318
	0.830	97.35	461	58.4	0.577
	0.860	105.9	466	-	-
	1.750	30.5	124	64.2	1.472
	2.150	22.2	87	66.0	0.864
	3.570	5.45	21	68.0	3.276
	3.000	10.6	40	-	-
4.290	4.1	16	67.5	3.998	
10 c/min	0.386	8.35	5255	51.2	0.184
	0.795	1.05	582	59.0	0.590
	0.860	1.25	734	59.0	0.655
	0.925	0.85	458	59.5	0.717
	0.600	2.55	1447	58.2	0.348
	1.29	0.55	290	63.4	1.016
	0.707	1.5	880	59.0	0.452

TABLE VII

Constant load amplitude push-pull fatigue tests
at variable stress ratios

Maximum compressive stress (t/in ²)	Maximum tensile stress (t/in ²)	Push-pull stress ratio (R)	Time to fracture, hr	Cycles to fracture
63.0	68.15	-0.925	4.3	18
63.0	68.15	-0.925	5.7	27
63.0	64.28	-0.975	24.0	109
58.0	63.0	-0.92	13.4	52
58.0	63.0	-0.92	14.6	55
63.0	63.0	-1.0	14.5	63
64.28	63.0	1.02	66.35	278
64.28	63.0	1.02	11.7	52
65.57	63.0	1.04	19.65	82
66.86	63.0	1.06	18.1	75
68.15	63.0	1.08	48.2	170
68.15	63.0	1.08	15.2	61
69.44	63.0	1.10	15.6	63
70.65	63.0	1.12	23.3	93
73.40	63.0	1.165	20.0	77

Tests conducted at ~7 c/hr

TABLE IV

Static constant tensile stress tests

Nominal applied stress (t/in ²)	True stress (t/in ²)	Time to failure (hr)
70.9	75.0	4.05
70.1	74.2	118.7
73.6	77.8	45.0
74.6	78.5	6.7
68.5	72.1	960 unbroken
68.0	72.4	0.75
70.2	74.6	3.5

TABLE V

Values of strain exponents

	Constant strain amplitude fatigue		Constant load amplitude fatigue	
	7 c/hr	10 c/min	7 c/hr	10 c/min
Total strain exponent (a)	0.405	0.407	0.275	0.288
Plastic strain exponent (k)	0.590	0.590	0.530	0.620

TABLE VI

Some characteristic load and strain values

Cycles to failure	Constant strain amplitude fatigue			Constant load amplitude fatigue		
	Applied strain range $\epsilon_T\%$	First cycle stress (t/in ²)	50% life stress (t/in ²)	First cycle strain $\epsilon_T\%$	50% life strain $\epsilon_T\%$	Maximum applied stress (t/in ²)
At 7 c/hr						
20	3.570	75.0	68.0	1.20	1.50	67.8
220	1.275	69.0	61.9	0.38	0.50	60.0
630	0.565	62.0	57.1	0.30	0.42	57.0
At 10 c/min						
400	0.925	62.5	59.5	0.27	0.62	60.4
900	0.707	62.5	59.0	0.42	0.62	58.0
5000	0.386	55.0	51.2	0.21	0.34	53.0

APPENDIX I

Definitions of terms used

The reader is sometimes confused by the indiscriminate use of fatigue jargon which is meaningful only to the specialist. Unfortunately, repeated explanations of terms and definitions can become lengthy and confuse the text. In order to clarify this Report, some of the more important terms which were described in previous work^{1,6,7} are redefined below.

The experimental programme was conducted in the low cycle (or high strain) fatigue range where failure is induced in less than or around 10^4 cycles. Under these conditions, the elastic range of the material is usually exceeded and the resulting strain is composed of elastic and plastic components such that stress, strain and load are no longer related by Young's modulus as in the elastic, Hookean range. The nature of the fatigue cycle is therefore dependent upon whether it is maintained at a constant stress, strain or load amplitude. The term 'load fatigue' refers to tests where the load amplitude is maintained constant whilst stress and strain are allowed to vary. Similarly, stress and strain fatigue are controlled off stress and strain respectively whilst the other parameters are allowed to vary. Typical inter-relations of stress, strain and load for the three forms of test are illustrated in Figure 13.

'Static loads' are those which are invariable with time, whereas 'cyclic loads' are, as the term implies, variable with time. Unfortunately, ultimate tensile strength values which are obtained from tests at a given stress or strain rate are sometimes referred to in the literature as static properties, despite the fact that they are produced under the application of incremental load, often applied at different rates during the test.

The term 'creep' is used to describe time-dependent strain, which may be produced by any type of test. The most common form of creep is that produced by a static load at elevated temperatures and this may be termed 'static creep'. The creep which can take place in some forms of fatigue loading has been referred to as either 'dynamic creep' or 'cyclic creep' by other authors in order to distinguish it from 'static creep'. 'Cumulative strain' is an alternative term which is used here in order to be more specific and to avoid confusion between the different forms of creep at elevated temperatures which are associated with specific deformation mechanisms. The simple definition of cumulative strain given in the text is the contemporary strain at maximum applied stress. This is a total strain which is composed of elastic and plastic components.

The 'strain range' is the difference between maximum and minimum strain in a given cycle. This term is usually used in the literature in preference to 'amplitude' which is used more specifically as the difference between zero and the maximum or minimum values.

In conventional fatigue the endurance limit is the stress below which life is infinite. 'Cyclic endurance' is used here to denote the number of cycles to failure for a given stress. 'Time to failure' refers

to the number of hours, and 'endurance' is a general term for describing either time or cycles.

The term 'repeated tension' is used to describe the case of zero minimum load and a tensile maximum load, and fully reversed push-pull is the case where the tensile and compressive maxima are equal and opposite. Compressive stresses are negative in sign and tensile stresses are positive. The push-pull stress ratio is the ratio of maximum compressive stress to maximum tensile stress. The mean stress is the stress midway between the respective stresses. For a mean stress of zero, the push-pull stress ratio is -1, and for a mean stress equal to half the maximum tensile stress (repeated tension) it is 0.

APPENDIX II

Strain/time analysis

The cumulative strain/time curves for push-pull fatigue at ~7 c/hr, illustrated in Figure 3, appeared on inspection to form a regular family similar to those exhibited by static tensile creep at elevated temperatures. The data are analysed by a formula originally developed for static stress creep by Graham⁹ which embodies the simple terms of primary and secondary creep (after Andrade) together with additional terms in the more comprehensive form:-

$$\epsilon = \epsilon_0 + \sum C\sigma^\beta t^\kappa \quad \dots(6)$$

The values of κ have been shown experimentally to vary according to stress and temperature and have discrete values which form the series ... $\frac{1}{27}$, $\frac{1}{9}$, $\frac{1}{3}$, 1, 3, 9 ... of which $\frac{1}{3}$ and 1 are present in Andrade's formula. The ratios of $\frac{\kappa}{\beta}$ are also discrete and are members of the series $\frac{1}{2}$, $\frac{1}{4}$, $\frac{1}{8}$, $\frac{1}{18}$... This flexible relation between stress, strain, and time, forms the first stage in a comprehensive analysis of creep-strain and rupture data for a range of temperatures, and it has been claimed to have been used successfully to describe and predict the behaviour of 178 sets of rupture data and 46 sets of creep data for a wide range of materials and temperatures¹⁶.

The data in Figure 3 were analysed by the first stage of this technique as described in Reference 10, the curves being separated into ϵ_0 , t^1 and t^9 components such that they were composed of three straight lines. The values of the t^1 and t^9 time intercepts at 1 per cent strain together with σ , ϵ_0 were as follows:-

σ t/in ²	ϵ_0 %	t^1 hr	t^9 hr
57.0	0.11	600	-
58.0	0.215	240	-
60.8	0.218	65	52
63.0	0.40	10.9	10.8
64.8	0.48	6.3	8.0
67.8	0.78	4.0	1.7

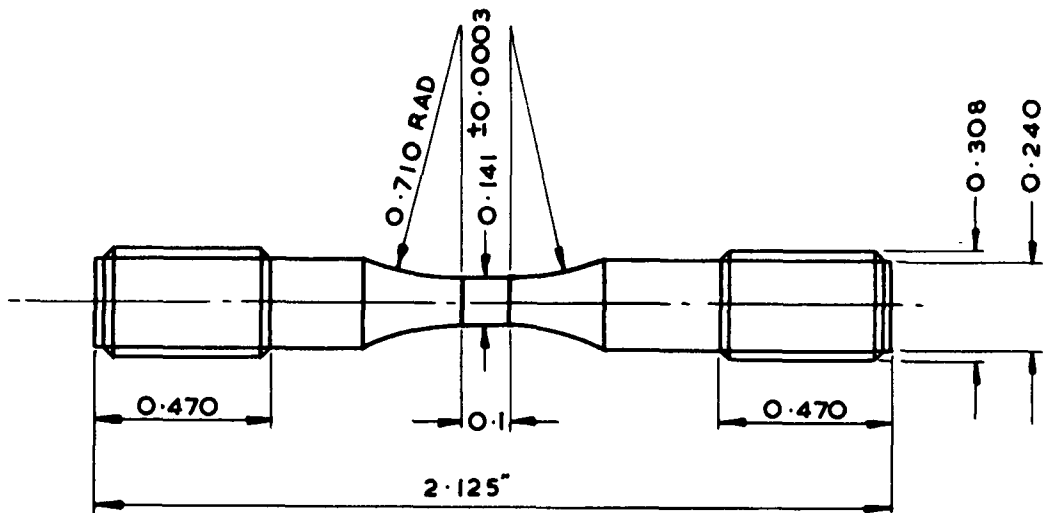
The t^1 and t^9 curves (stress against the time intercepts at 1 per cent strain) were plotted in Figures 10.1 and 10.2, and the data were

described by straight lines of slopes $\left(\frac{k}{\beta}\right)$ close to $-\frac{1}{32}$ (Figure 10). The stresses were plotted against ϵ_0 (Figure 10.3) and again the data could be described by a straight line, in this case of slope $\sim\frac{1}{12}$. This curve was of course a section of the virgin stress/strain curve because each numerical value of ϵ_0 was in fact the tensile strain reached in the first quarter cycle, where tension was always applied first.

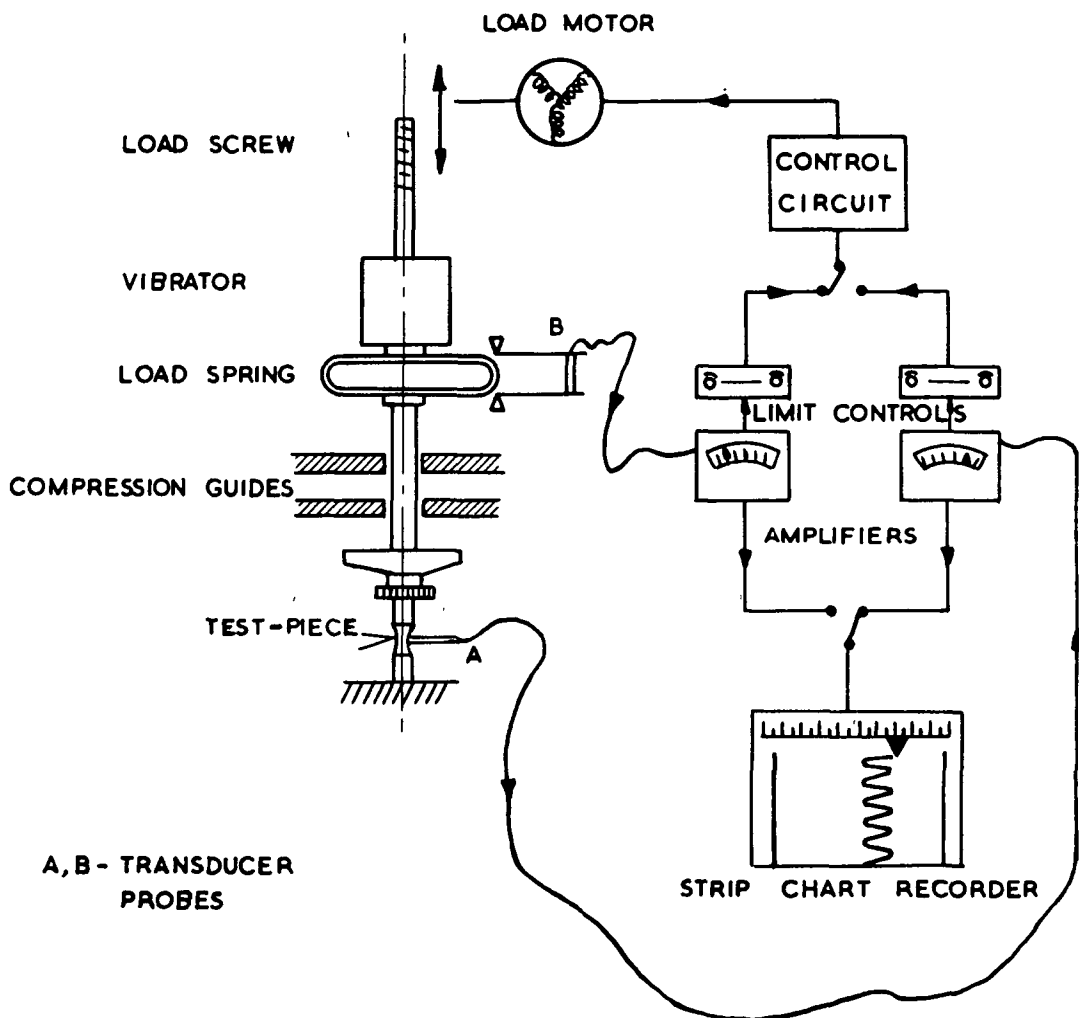
The ϵ/t curves were regenerated from the 'theoretical' ϵ_0 , t^1 and t^9 time intercepts from Figures 10.1, 10.2 and 10.3, and were represented in Figure 11 as broken curves. The accuracy of this analysis may be estimated by comparing the closeness of the respective experimental points to the regenerated curves.

The closeness of the fit of the theoretical curves to the experimental push-pull strain accumulation suggests that such data can be described adequately by the general formula. This is surprising at first sight, because in general, the mechanical processes that produce deformation are characteristic of the testing temperature, and differ at high and low temperatures. The mechanisms that produced the strain/time curves analysed here would not be expected to be the same as those that produce static creep for this material at say 600°C therefore. In addition, push-pull is an obviously different condition from either repeated or static tension because the direction of loading is repeatedly reversed and the Bauschinger effect becomes operative. This apparent similarity between the mathematical forms of the respective creep and fatigue ϵ/t curves appears to be a significant addition to the applicability of the general equation. Additional work will be conducted in a future programme on push-pull at elevated temperatures to examine further the efficacy of the technique and to determine whether the time-temperature parameters fit the data over a temperature range that is sufficiently wide to include room temperature as well as conventional creep. Conversely, it will be interesting to examine such departures from the 'normal' creep behaviour as may occur with temperature, and whether they can be related by metallographic examinations to the changing mechanisms of deformation.

FIG. 1

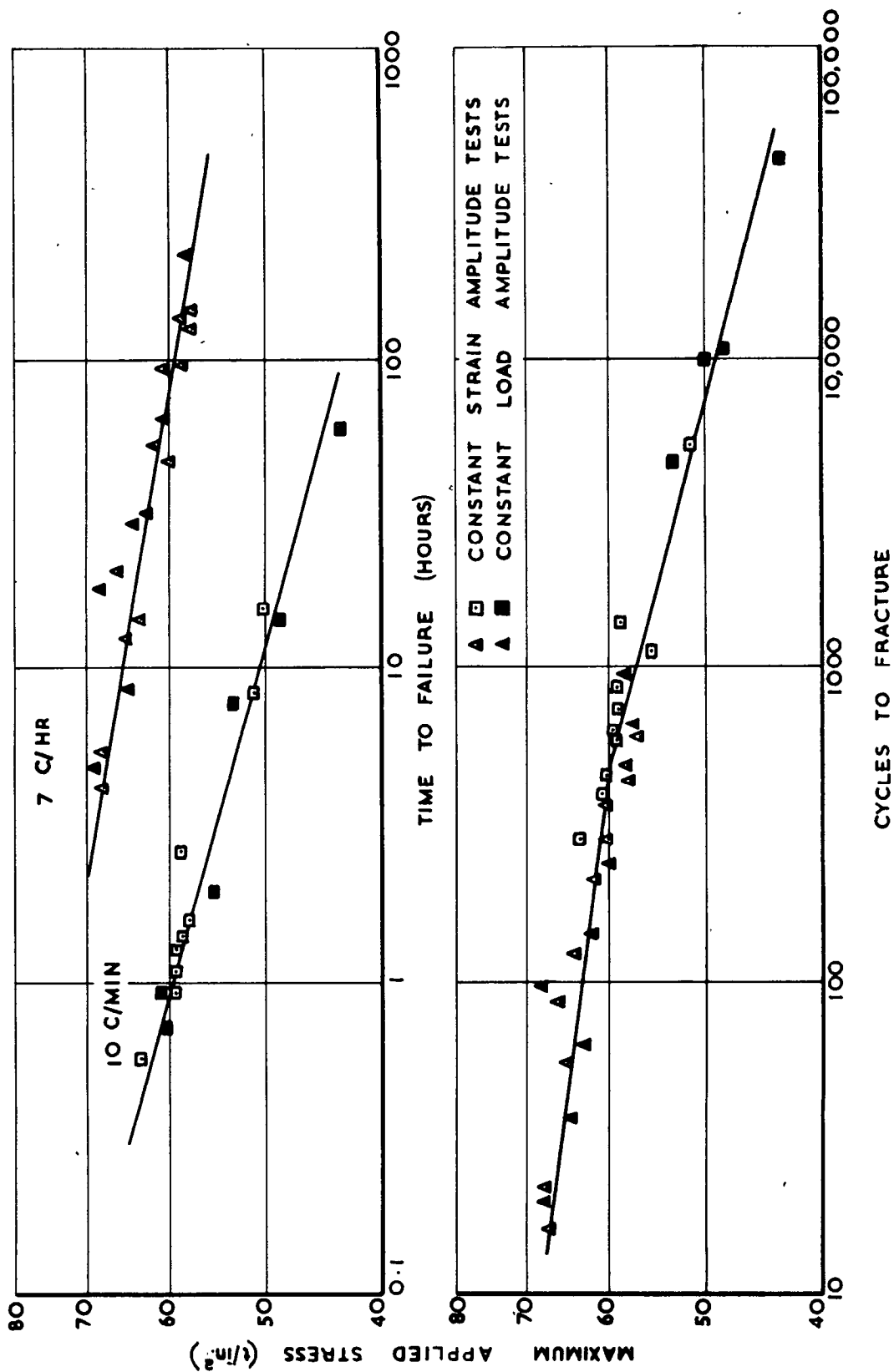


1.1 ROOM TEMPERATURE PUSH/PULL FATIGUE TEST-PIECE



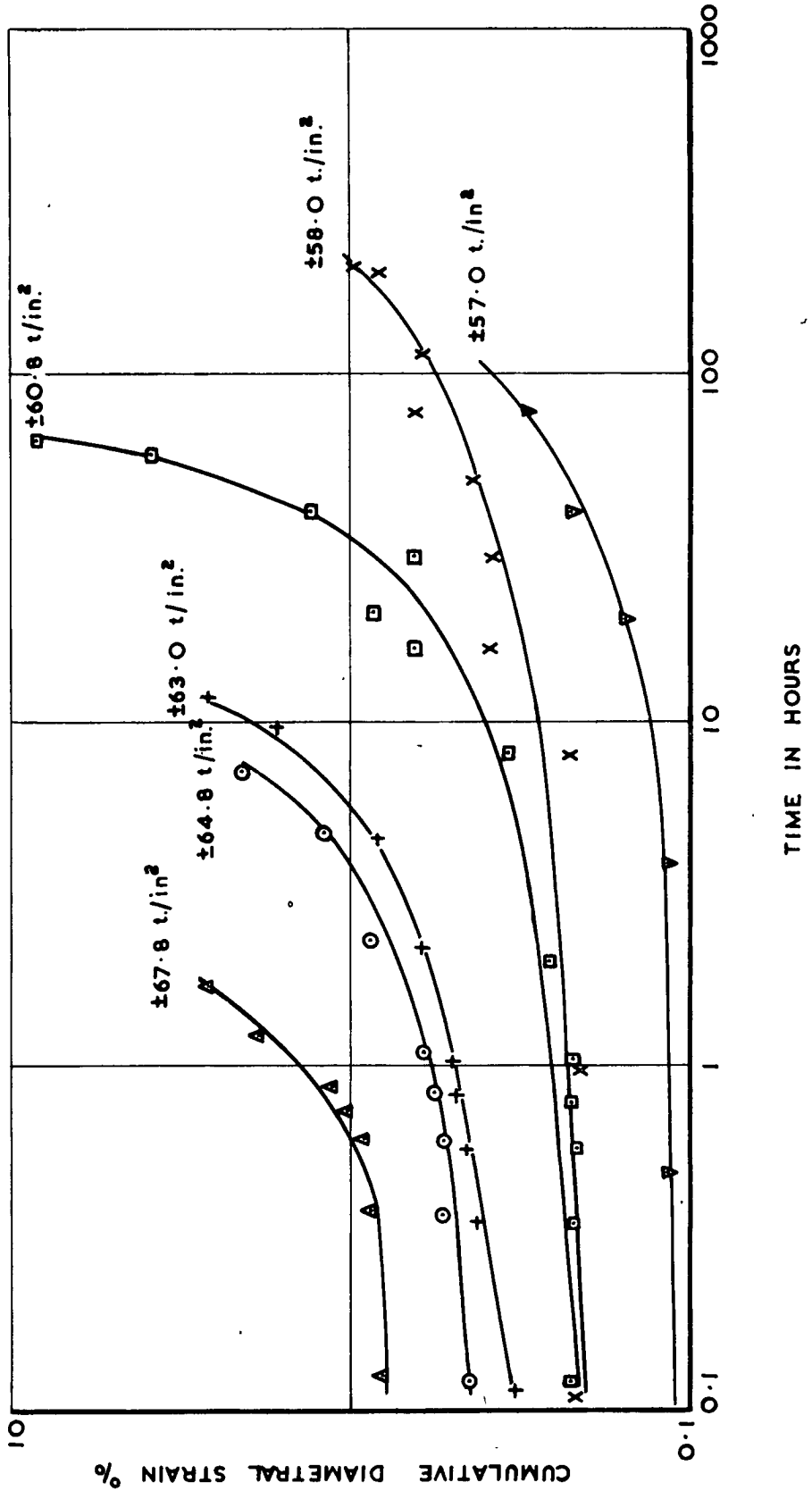
1.2 SCHEMATIC DIAGRAM TO SHOW SYSTEM FOR THE CONTROL AND RECORDING OF THE SLOW FATIGUE

FIG. 2



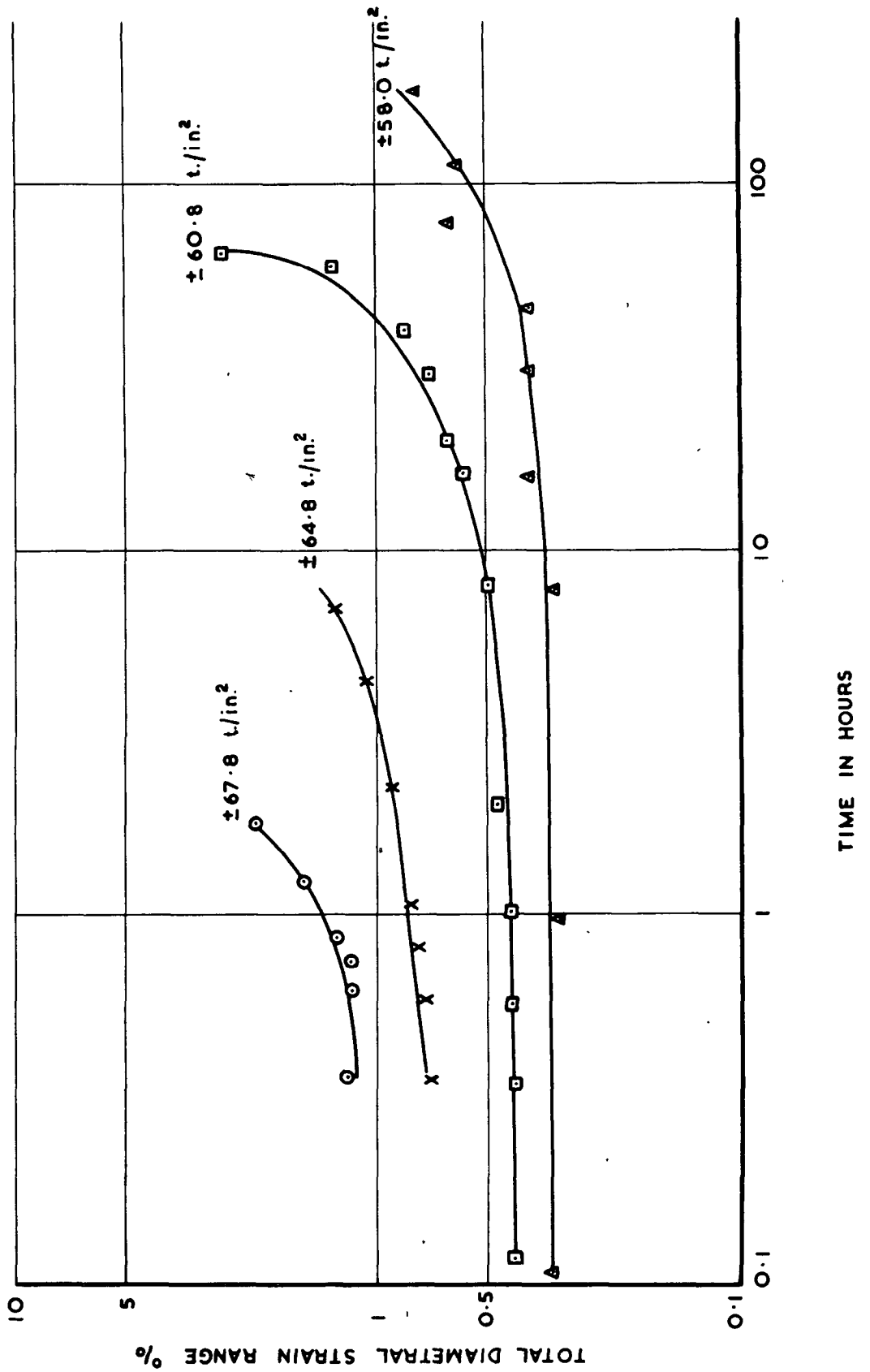
CONSTANT LOAD AND CONSTANT STRAIN
AMPLITUDE FATIGUE STRESS/TIME
RUPTURE CURVES

FIG. 3

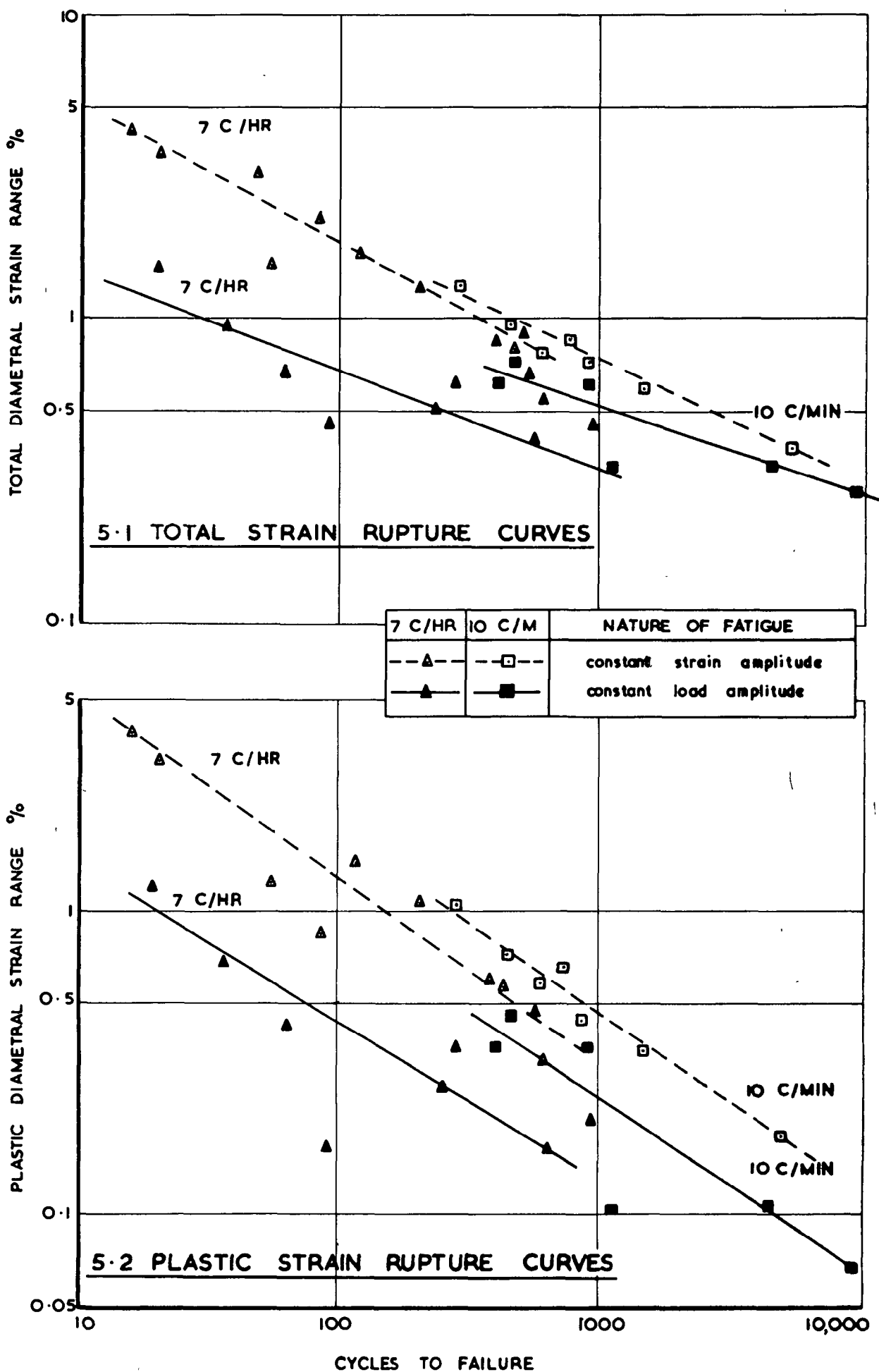


CUMULATIVE STRAIN/TIME CURVES FOR
PUSH/PULL FATIGUE AT 7 C/HR

FIG. 4

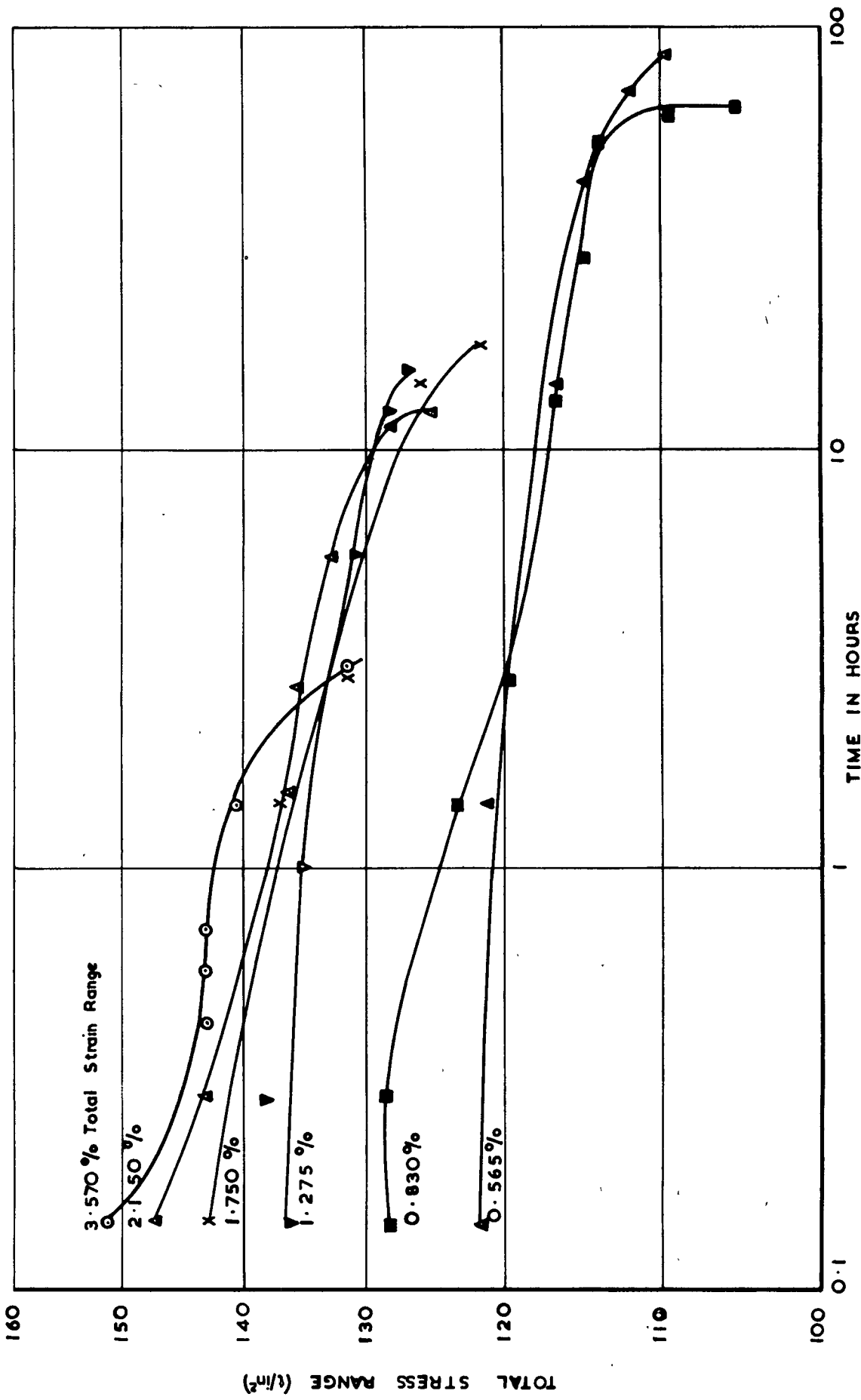


TOTAL STRAIN RANGE / TIME CURVES FOR PUSH/PULL FATIGUE AT 7 C/HR.



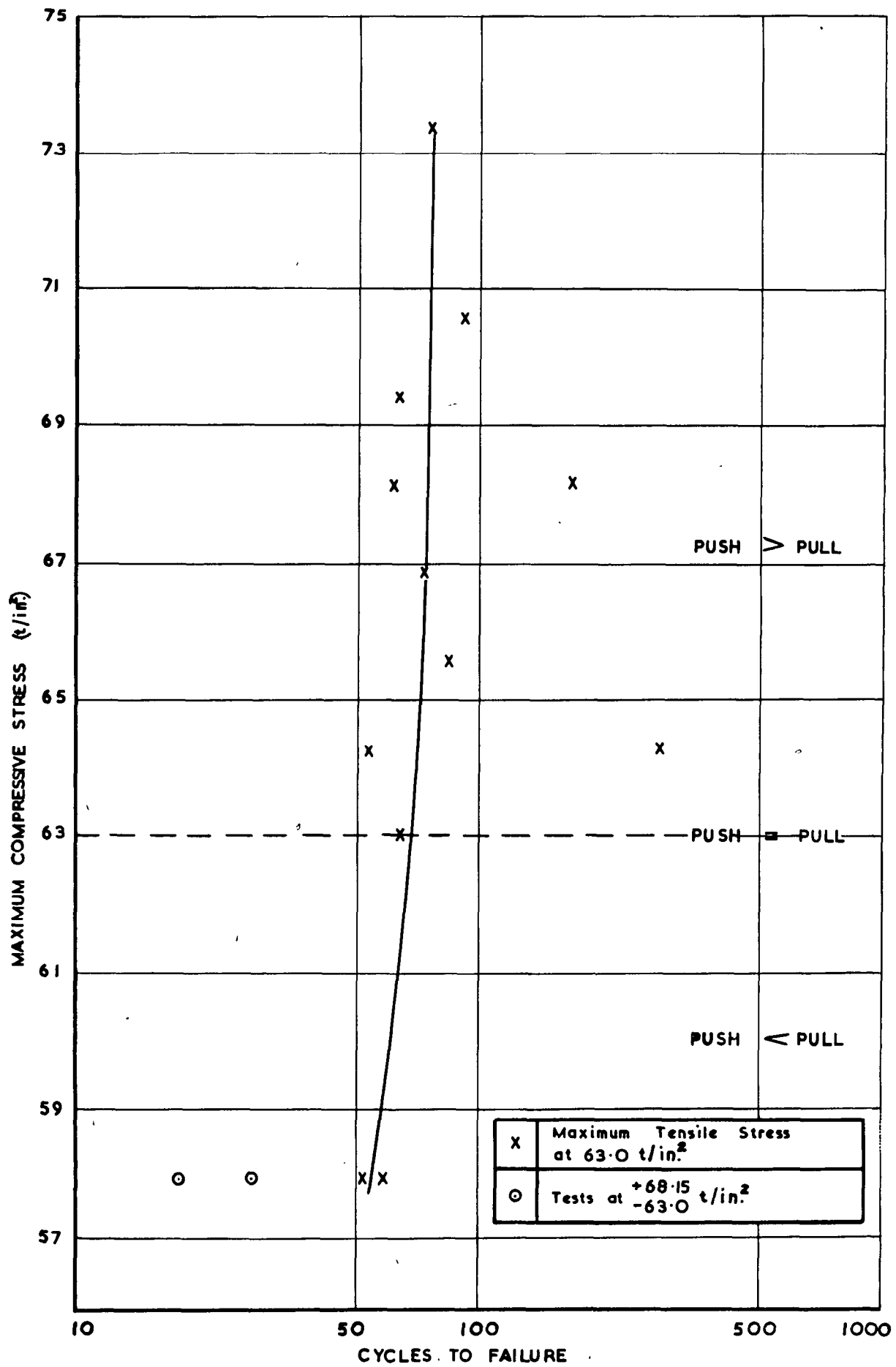
TOTAL AND PLASTIC STRAIN/CYCLES
RUPTURE CURVES

FIG. 6



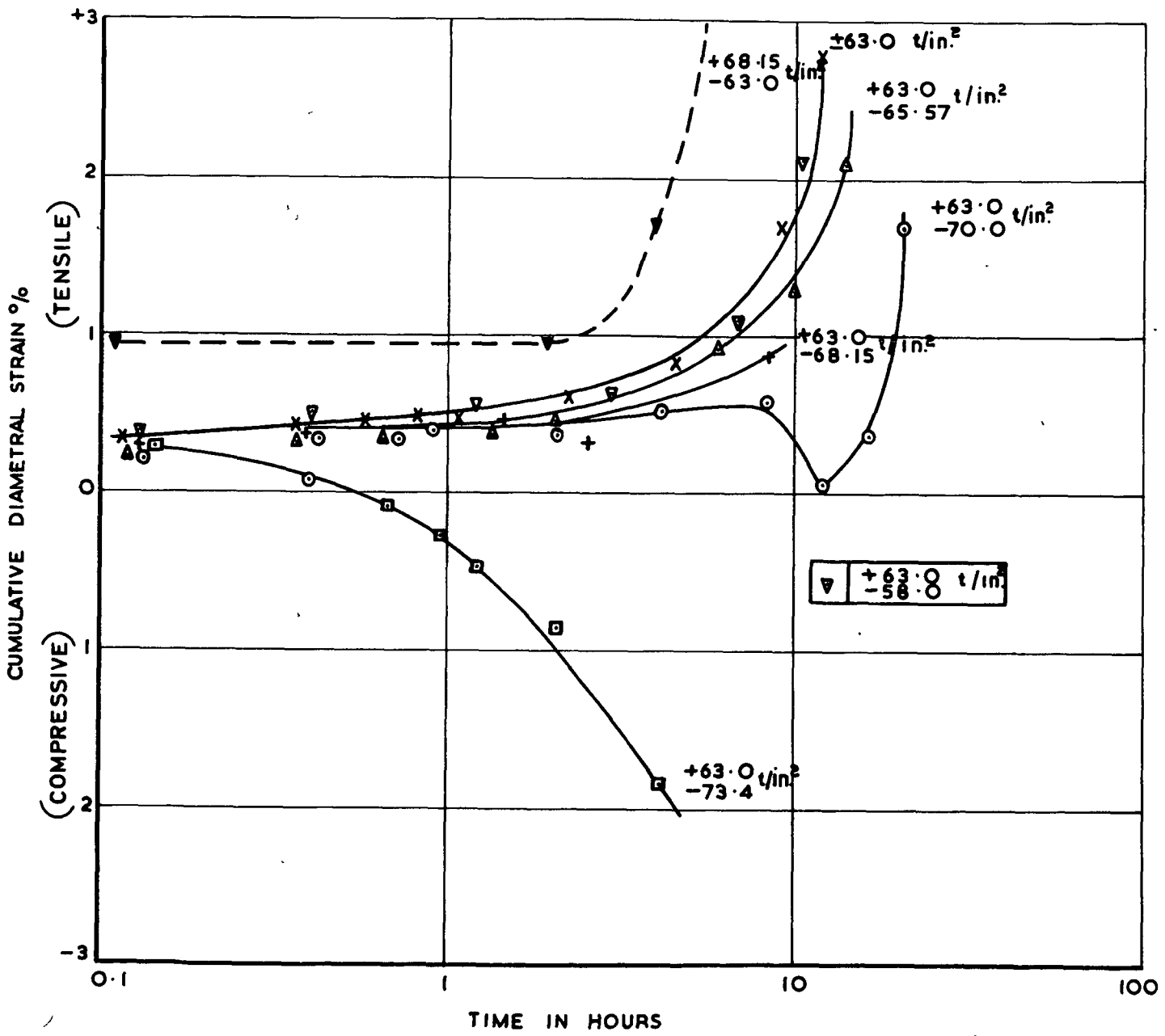
RELAXATION OF TOTAL STRESS RANGE
DURING CONSTANT STRAIN AMPLITUDE
FATIGUE TESTS AT 7 C/HR

FIG. 7



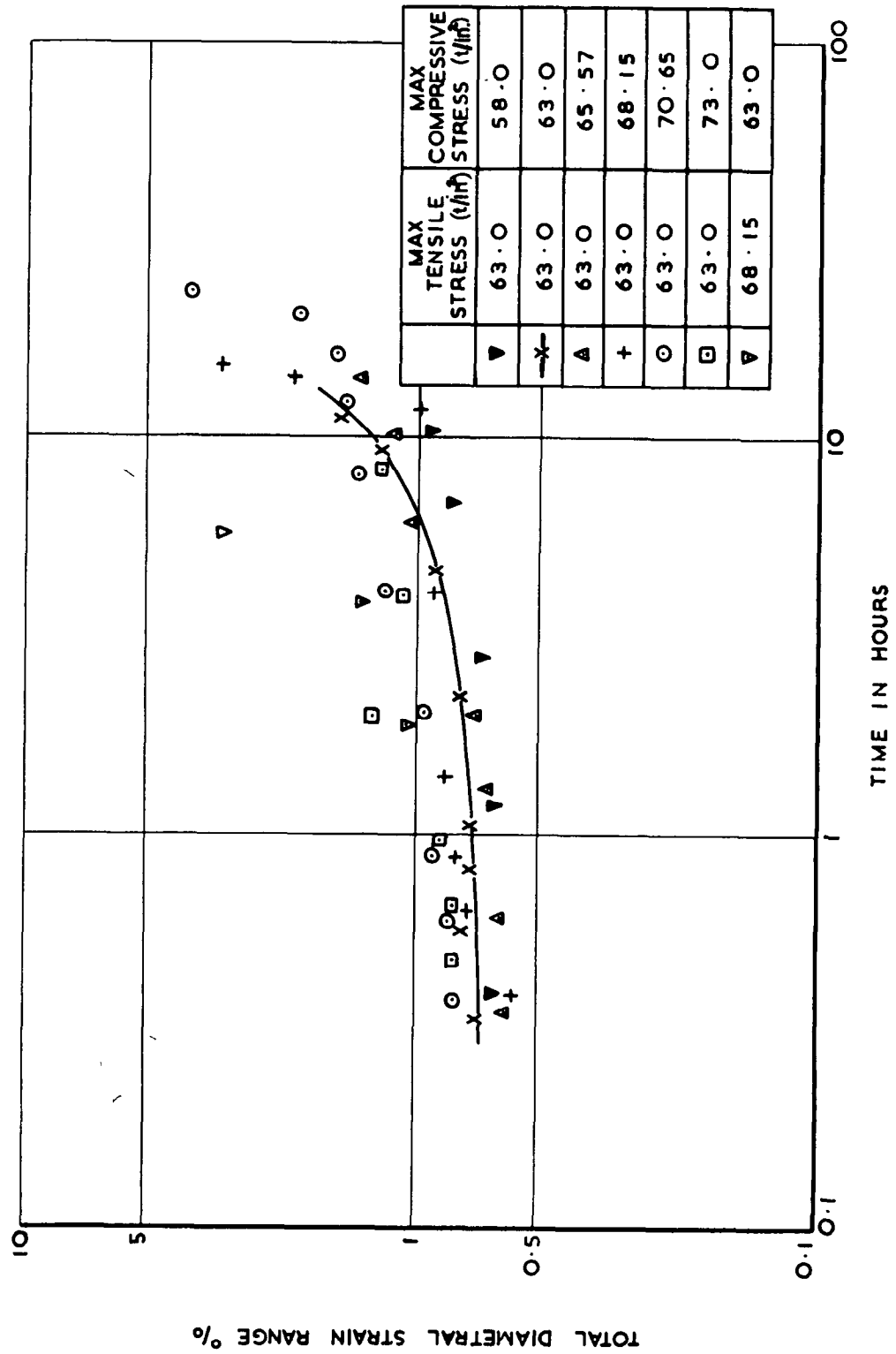
EFFECT OF VARIATION OF PUSH/PULL
STRESS RATIO ON FATIGUE ENDURANCE
AT 7 C/HR.

FIG. 8



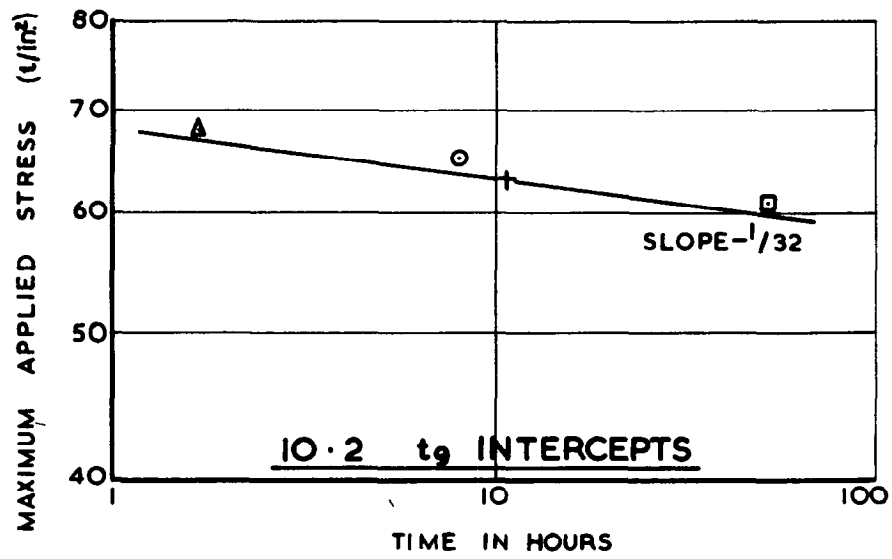
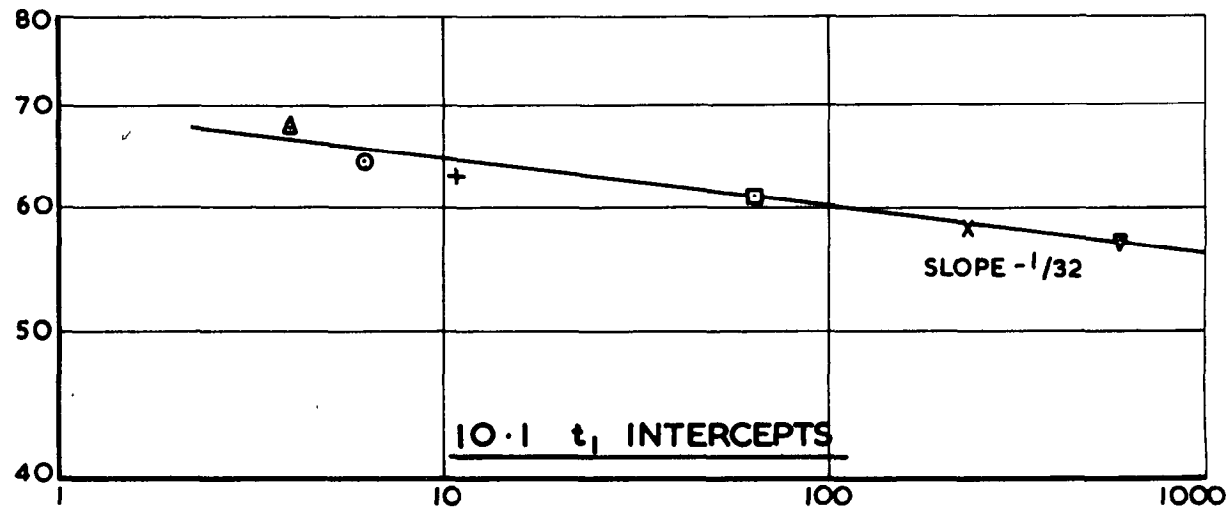
EFFECT OF VARIATION OF PUSH/PULL STRESS RATIO ON THE CUMULATIVE STRAIN/TIME CURVES AT 7 C/HR

FIG. 9

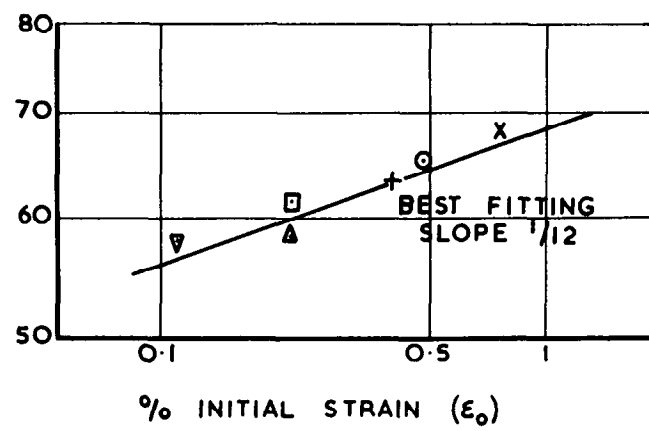


EFFECT OF VARIATION OF PUSH/PULL RATIO
ON TOTAL STRAIN RANGE/TIME CURVES

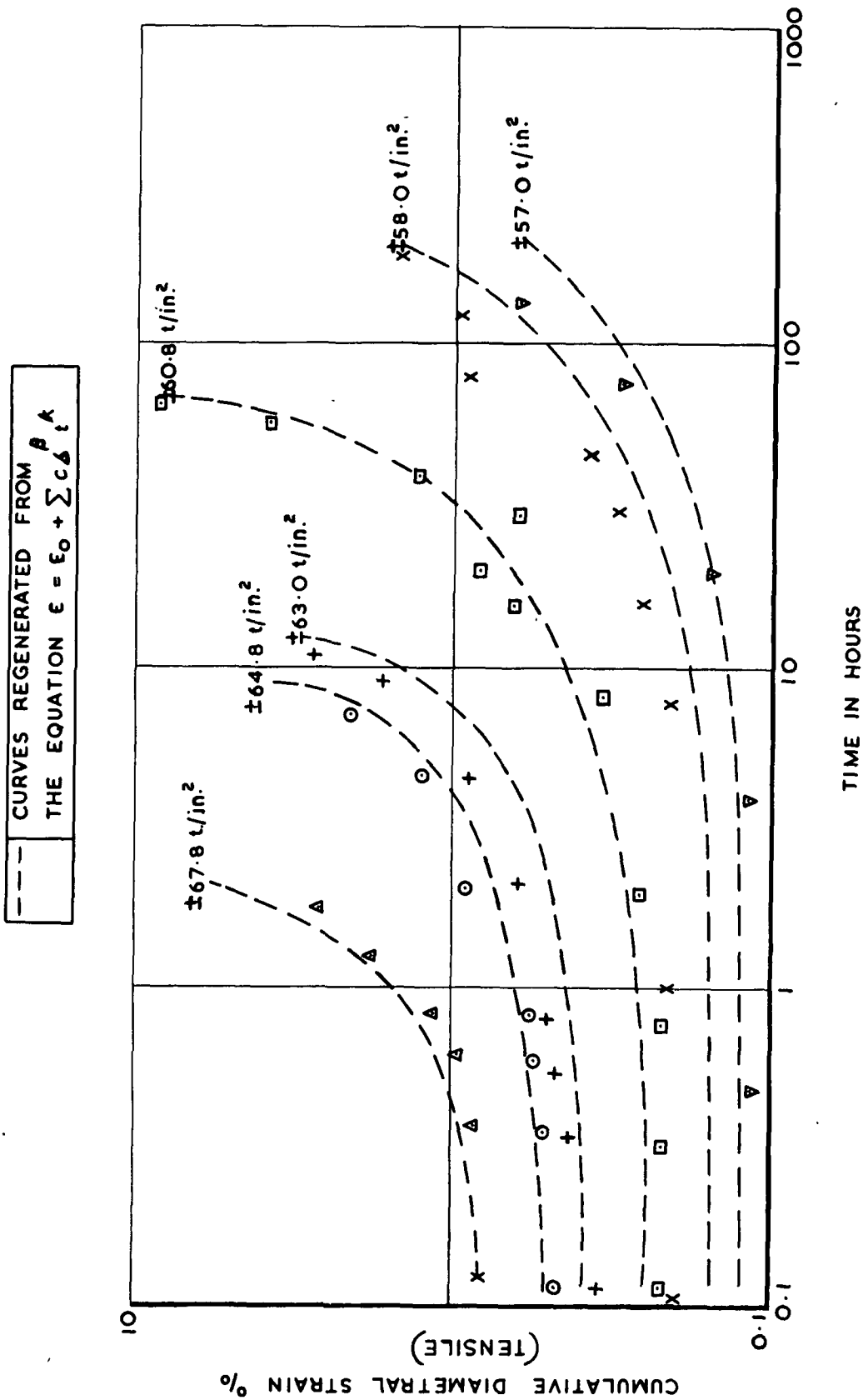
FIG. 1



∇	57.0 t/in^2
x	58.0 t/in^2
\square	60.0 t/in^2
+	63.0 t/in^2
\circ	64.8 t/in^2
Δ	67.8 t/in^2

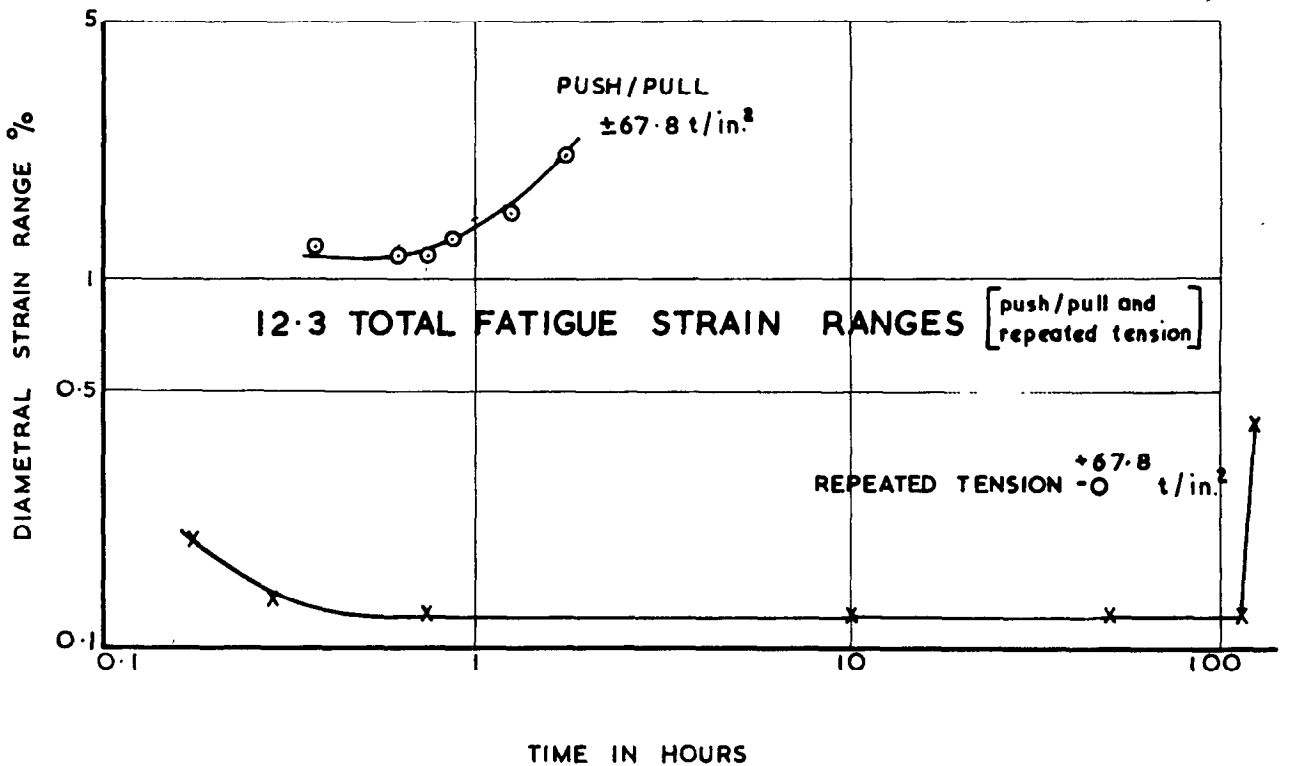
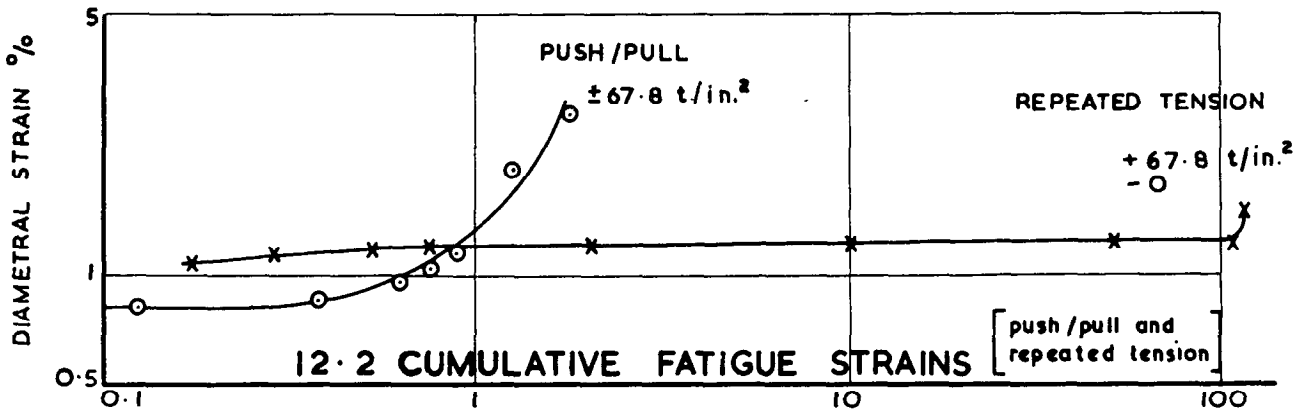
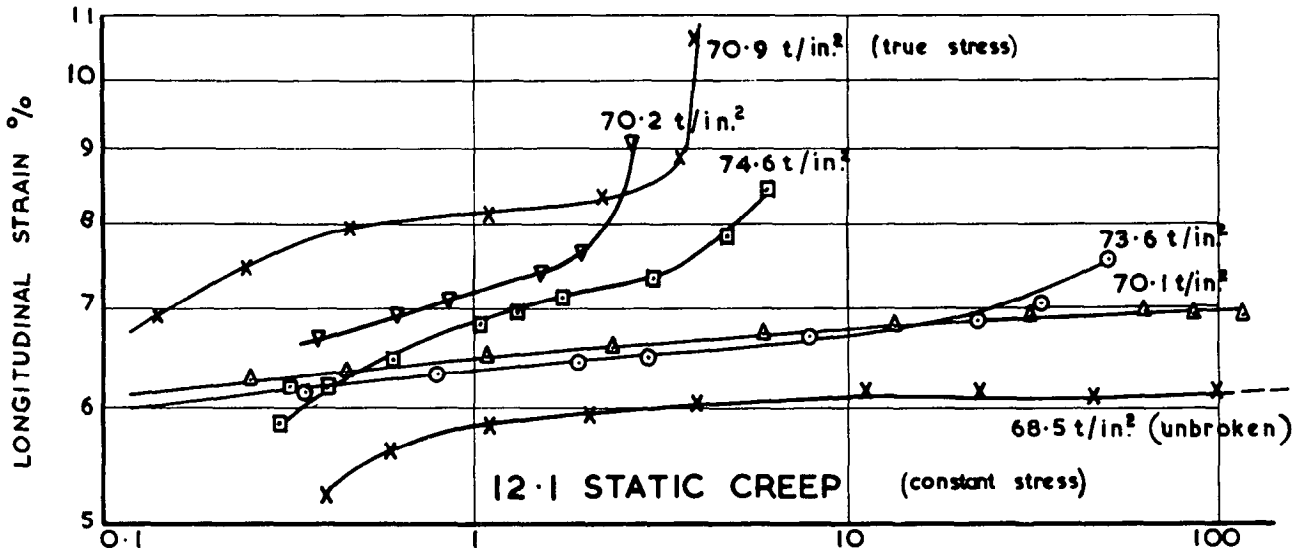


t_1 t_9 AND ϵ_0 CROSS-PLOT CURVES

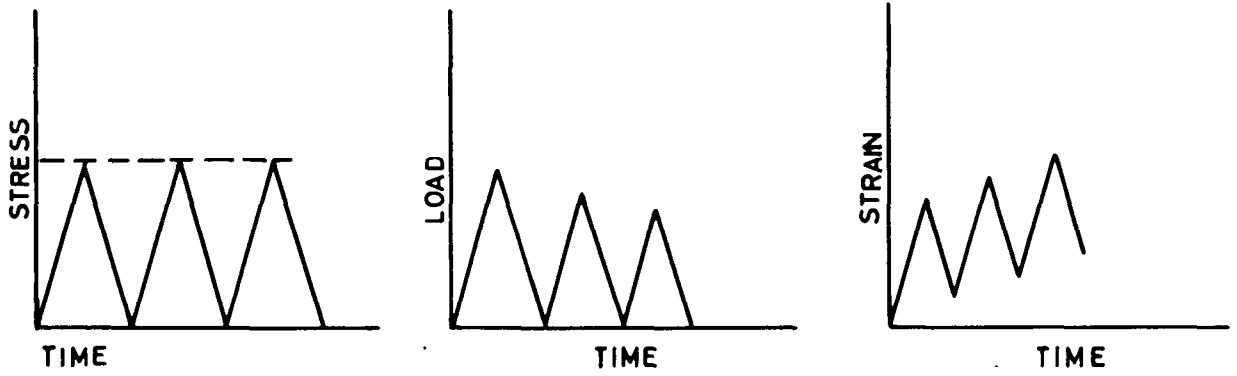


RE-GENERATED STRAIN/TIME CURVES FITTED TO EXPERIMENTAL DATA

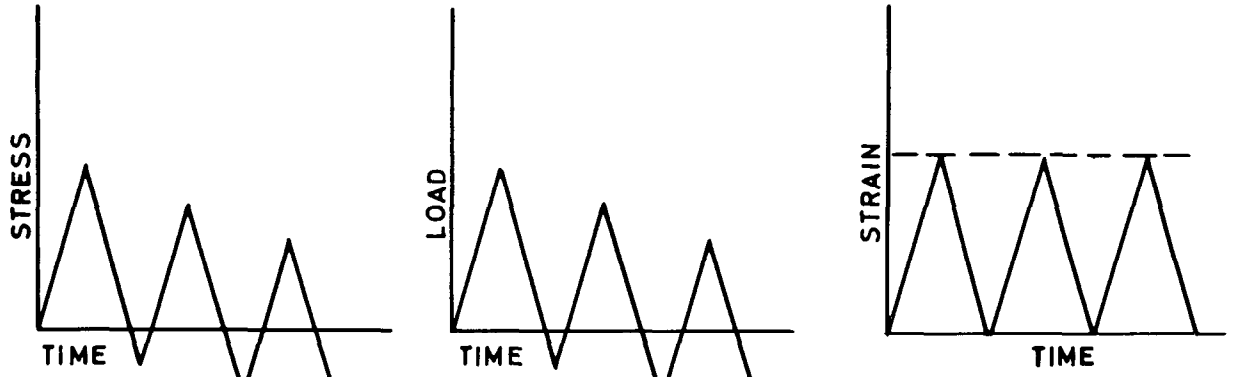
FIG. 12



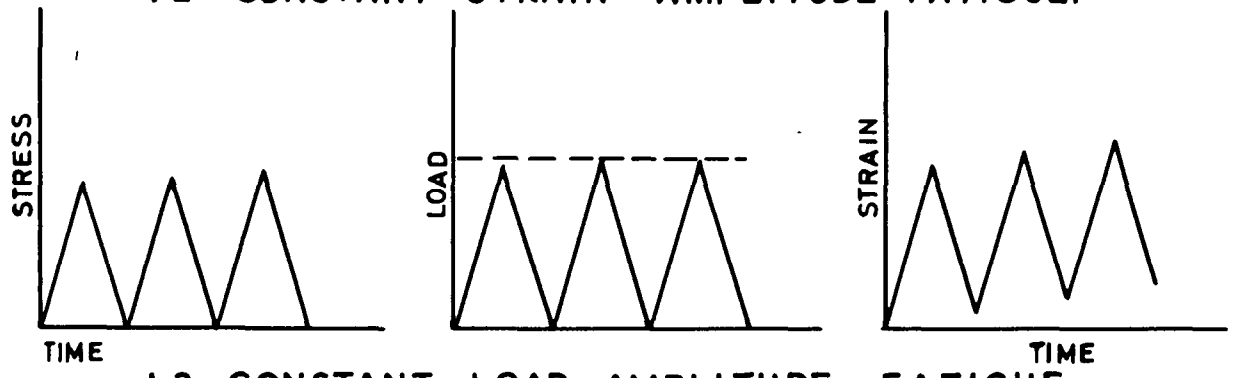
CREEP AND FATIGUE CUMULATIVE STRAIN/TIME CURVES



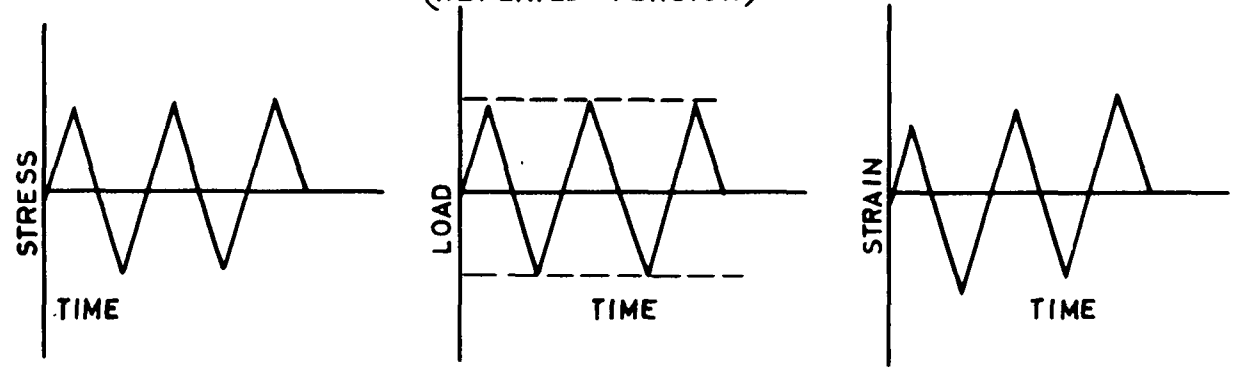
1.1 CONSTANT STRESS AMPLITUDE FATIGUE.



1.2 CONSTANT STRAIN AMPLITUDE FATIGUE.



**1.3 CONSTANT LOAD AMPLITUDE FATIGUE.
(REPEATED TENSION)**



**1.4 CONSTANT LOAD AMPLITUDE FATIGUE.
(PUSH-PULL)**

**THE BEHAVIOUR OF STRESS STRAIN
AND LOAD DURING HIGH STRESS
FATIGUE OF H46.**

A.R.C. C.P. No. 844

539.431:669.15.26-194

THE ROLE OF COMPRESSIVE STRESS IN THE LOAD AND STRAIN
FATIGUE BEHAVIOUR OF H.46 AT ROOM TEMPERATURE

TILLY, G. P. JUNE 1965

Constant load amplitude and constant strain amplitude fatigue tests have been conducted on an 11 per cent Cr steel (H.46) at frequencies of 7 c/hr and 10 c/min at room temperature. The rupture data of the two tests correlated closely for both frequencies in terms of maximum applied stress at 50 per cent life, but the constant strain amplitude data exhibited enhanced endurance in terms of strain range at this life. In general, constant load amplitude fatigue appeared to be more damaging than constant strain at this temperature.

The constant load amplitude fatigue tests accumulated tensile strain in a time dependent manner which was amenable to analysis by a technique originally developed for elevated temperature creep data. The

P.T.O.

A.R.C. C.P. No. 844

539.431:669.15.26-194

THE ROLE OF COMPRESSIVE STRESS IN THE LOAD AND STRAIN
FATIGUE BEHAVIOUR OF H.46 AT ROOM TEMPERATURE

TILLY, G. P. JUNE 1965

Constant load amplitude and constant strain amplitude fatigue tests have been conducted on an 11 per cent Cr steel (H.46) at frequencies of 7 c/hr and 10 c/min at room temperature. The rupture data of the two tests correlated closely for both frequencies in terms of maximum applied stress at 50 per cent life, but the constant strain amplitude data exhibited enhanced endurance in terms of strain range at this life. In general, constant load amplitude fatigue appeared to be more damaging than constant strain at this temperature.

The constant load amplitude fatigue tests accumulated tensile strain in a time dependent manner which was amenable to analysis by a technique originally developed for elevated temperature creep data. The

P.T.O.

A.R.C. C.P. No. 844

539.431:669.15.26-194

THE ROLE OF COMPRESSIVE STRESS IN THE LOAD AND STRAIN
FATIGUE BEHAVIOUR OF H.46 AT ROOM TEMPERATURE

TILLY, G. P. JUNE 1965

Constant load amplitude and constant strain amplitude fatigue tests have been conducted on an 11 per cent Cr steel (H.46) at frequencies of 7 c/hr and 10 c/min at room temperature. The rupture data of the two tests correlated closely for both frequencies in terms of maximum applied stress at 50 per cent life, but the constant strain amplitude data exhibited enhanced endurance in terms of strain range at this life. In general, constant load amplitude fatigue appeared to be more damaging than constant strain at this temperature.

The constant load amplitude fatigue tests accumulated tensile strain in a time dependent manner which was amenable to analysis by a technique originally developed for elevated temperature creep data. The

P.T.O.

rate of strain accumulation of repeated tension load fatigue and static tensile stress tests was slower than for fully reversed push-pull. Strain continued to accumulate in a tensile sense during push-pull tests at 7 c/hr despite excess compressive stresses which were as much as 8 per cent greater than the complementary tensile stresses, whilst cycles with 16.5 per cent excess compressive stress produced compressive strain accumulation. Repeated tension fatigue work-hardened the material and it became successively more resistant to deformation, whereas push-pull fatigue work-softened it and it became successively less resistant to deformation.

rate of strain accumulation of repeated tension load fatigue and static tensile stress tests was slower than for fully reversed push-pull. Strain continued to accumulate in a tensile sense during push-pull tests at 7 c/hr despite excess compressive stresses which were as much as 8 per cent greater than the complementary tensile stresses, whilst cycles with 16.5 per cent excess compressive stress produced compressive strain accumulation. Repeated tension fatigue work-hardened the material and it became successively more resistant to deformation, whereas push-pull fatigue work-softened it and it became successively less resistant to deformation.

rate of strain accumulation of repeated tension load fatigue and static tensile stress tests was slower than for fully reversed push-pull. Strain continued to accumulate in a tensile sense during push-pull tests at 7 c/hr despite excess compressive stresses which were as much as 8 per cent greater than the complementary tensile stresses, whilst cycles with 16.5 per cent excess compressive stress produced compressive strain accumulation. Repeated tension fatigue work-hardened the material and it became successively more resistant to deformation, whereas push-pull fatigue work-softened it and it became successively less resistant to deformation.

© *Crown copyright 1966*

Printed and published by

HER MAJESTY'S STATIONERY OFFICE

To be purchased from

49 High Holborn, London w.c.1

423 Oxford Street, London w.1

13A Castle Street, Edinburgh 2

109 St. Mary Street, Cardiff

Brazennose Street, Manchester 2

50 Fairfax Street, Bristol 1

35 Smallbrook, Ringway, Birmingham 5

80 Chichester Street, Belfast 1

or through any bookseller

Printed in England